

Buckling of Cracked Conical Frusta under Axial Compression

Dadrasi Ali

Department of Mechanics, Shahrood Branch, Islamic Azad University, Shahrood, IRAN

Available online at: www.isca.in

Received 28th September 2012, revised 3rd October 2012, accepted 6th November 2012

Abstract

Presence of cracks or similar imperfections can considerably reduce the buckling load of a shell structure. In this paper, the buckling of thin conical frusta with cracks under axial loads has been studied. At first, a frustum without any imperfection has been analyzed. In continuation, sensitivity of the buckling load to the crack presence with different length and orientation has also been investigated. This procedure has been investigated on three types of frusta with different heights and constant semi-apical angles. Some effective parameters on buckling have been studied separately and the required data for analysis have been gained through experimental tests. The finite element ABAQUS software has been used for the numerical analyses.

Key words: Buckling, frusta, crack, FEM.

Introduction

Shell structures have been widely used in many fields like pipelines, aerospace and marine structures, large dams, shell roofs, liquid-retaining structures and cooling towers¹. Shell's buckling is one of the important considerations within designing this structures²⁻³. Presence of defects, such as cracks, may seriously compromise their buckling behavior and endanger the structural integrity⁴⁻⁶. The post-buckling analysis of cracked plates and shells showed that the buckling deformation could cause a considerable amplification of the stress intensity around the crack tip⁷. On the other hand, increasing the load can cause propagation of the local buckling leading to the catastrophic failure of the structure⁸. The nonlinear buckling of thin cylindrical shells with longitudinal cracks subject to above-mentioned loading was studied by Starnes and Rose⁹⁻¹⁰. It was concluded that the non-linear interaction between in-plane stress resultants and the out-of-plane displacements near a crack significantly affects the buckling behavior of the shells. These studies indeed revealed that the sensitivity of the buckling behavior of both plates and shells to the presence of defects highly depends on the loading condition. As an example, Estekanchi et al.¹¹⁻¹² showed the buckling behavior of the cylindrical shells under torsional loading is less sensitive to the presence of a crack than that of a similar axially compressed cylindrical shell. Postlethwaite and Mills¹³ performed the axial crushing of conical shells of semi-apical angles ranging from 5° to 20° and studied their energy absorption capacity. Mamalis and Johnson¹⁴ have studied the axial compression of aluminium conical frusta of semi-apical angles from 5° to 10° under quasi-static loading. Mamalis et al.¹⁵ have also performed the axial compression on steel thin-walled frusta of semi-apical angles from 5° to 10° at elevated strain rates. The load-deformation behavior and the collapse in this case were similar to those in¹⁴.

With respect to Presented papers, it's observed that the category

of crack presence in frusta despite of its importance hasn't been probed up to now. In this paper, the effect of crack presence with different angles on the buckling behavior of various types of conical thin frusta has been investigated.

Material and Methods

Figure 1 shows the total geometry of specimens. In all of cones, the large diameter is $D=50\text{mm}$ and the semi-apical angle is $\Theta=4.5^\circ$ and both of these parameters are constant. Also, the center of crack is laid in the middle of cone's height. Crack lengths are $a=10, 20$ and 30 mm that have been analyzed with angles $\Theta=0^\circ, 30^\circ, 60^\circ$ and 90° and the shell's thickness is considered 1mm. The mechanical properties of the investigated steel shells have been obtained through the standard tensile test ASTM E8 and an INSTRON 8802 servohydraulic machine. It's stress-strain curve has been displayed in figure 2. The obtained elasticity modulus from linear elastic region is equal to $E=201$ GPa. Moreover the Poisson's ratio is set equal to $\nu=0.3$.

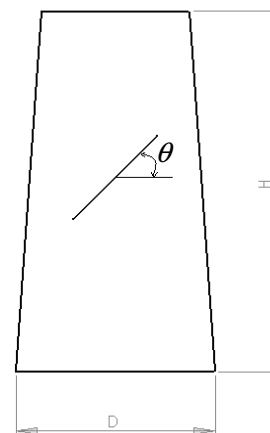


Figure-1
The total geometry of specimens

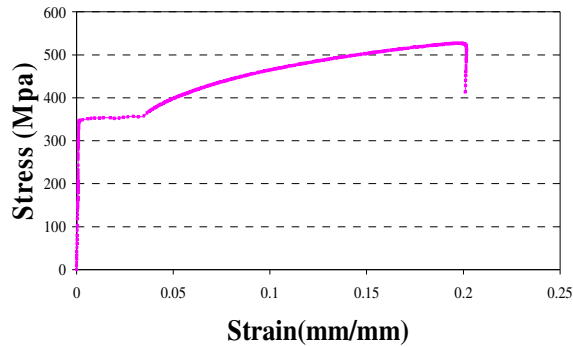


Figure-2

The stress-strain curve resulted by the experimental test

The data of the plastic region of the stress-strain curve has been used for the analysis of the plastic behavior in ABAQUS software. The shells have been laid under axial compression by means of supports that prepare clamp boundary condition.

Finite element analysis: FE methods are considered to be the most appropriate tool in cases dealing with structural mechanics problems involving complications in behavior that are analytically intractable. Buckling of cracked shells is such a problem. FE methods have been successfully applied in problems involving shell buckling and cracked shells¹².

In shell buckling problems, adequacy of the FE mesh for incorporating the shell buckling modes, which is sometimes unexpectedly complicated, is of utmost importance. Failing to observe this condition can result in omission of the first few buckling modes and grossly overestimated buckling loads. Shell structures usually buckle in complex modes relative to their initial geometry. Therefore, the analyst should resort to past experience and empirical rules for selecting an appropriate FE mesh in the buckling analyses. Numerous shell element formulations are available for buckling and large displacement analysis. Among them, popular isoparametric formulations seem to be most convenient and reliable in general applications. Quadrilateral elements are usually recommended for problems involving buckling behavior. In cracked plate and shell problems, appropriate modeling of the singular stress field at the crack tip area is of prime importance.

The numerical simulations were carried out using the general finite element program ABAQUS 6.6.3. At first we must do the meshing in order that we can analyze the specimen. The nonlinear element S8R5, which is suitable for analysis of thin shells, was used¹⁶. This element is an eight-node element with five-degree of freedom including three displacements in three directions of the coordinate axes and two rotations for each node. Figure 3 shows a meshed specimen with horizontal crack. We should change meshing so much that we reach an optimized meshing. That is, we should continue meshing to the extent that there isn't any considerable difference in buckling load coefficient that is achieved by linear analysis. Linear analysis must be done for getting eigenvalue by using the Buckle solver in ABAQUS software and getting the buckling modes. These

modes have smaller eigenvalues and buckling usually occurs in these mode shapes. Of course we should notice that eigenvalue analysis overestimates the value of buckling load, because in this analysis, we don't consider the plastic properties of material. In continuation, considering the plastic properties of material, a non-linear analysis is done by using Static Risks solver. Then, in this analysis, we take into consideration the effect of mode shapes of buckling gotten from the linear analysis. Figure 4 shows crack tip meshing. As a result a load-displacement curve is obtained and the maximum value of this curve displays the buckling load.

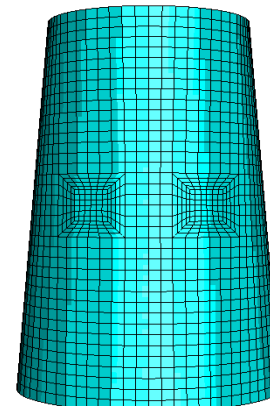


Figure-3

Meshed specimen with H=100 mm and a=20 mm

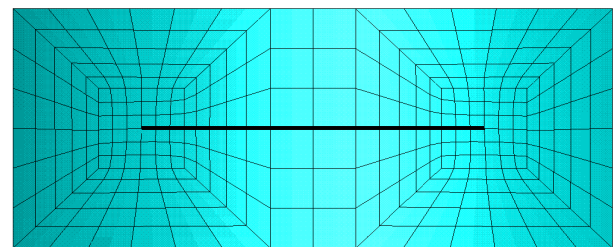


Figure-4

Meshing the tip of the crack

The point that should be considered in this analysis is the imperfection in the shells. Shells mainly due to their construction don't follow the ideal shape of a cone. This deviation from the ideal shape must be considered in the analysis. For example, about conical shells which are produced through the process of drawing because of fluidizing material during the process of forming, some small waves are created on the shell that make it out of ideal shape. Usually, in the shells, the imperfection is considered about 0.02th of its thickness¹⁶.

In the cracked conical shell, the occurrence of buckling phenomenon is more likely in these two positions. The first position is in which shell has the minimum diameter, and the second position is in which shell has the lowest strength because of the presence of crack in the shell. Now considering how stress is distributed in the shell and which area will be yielded soon, the buckling is occurred. Even the geometry of shell and crack and also stress distribution may be in such a way that both areas are yielded.

Results and Discussion

Analysis of shells 75mm in height: At first, conical shells with D: 50mm, H: 75mm, and semi-apical angle of 4.5° are analyzed. One uncracked sample of this cone has buckling load equal to 43.168kN. Now if we create a horizontal crack with the length of $a=10\text{mm}$, the amount of 0.65kN of shell buckling load is reduced. Figure 5 demonstrates the buckling of a sample with mentioned characteristics. As you notice in this figure, buckling has been occurred in the necking part of shell and a plastic ring on the top of shell has been created symmetrically. The point that is clear in distributing stress of these shells is the fact that by increasing loading, severe stress concentration is created in both crack tips which in continuation, more severe stress concentration is created in necking part of shell that finally can lead to yielding of shell in that part.

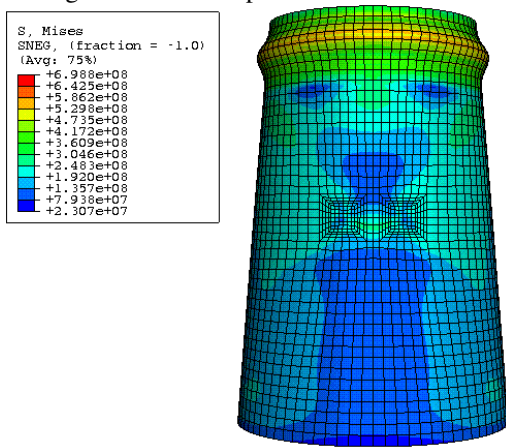


Figure-5

Distributing stress in a shell with $a=10\text{ mm}$ and $\Theta=0^\circ$

In continuation, we rotate the angle of crack $a=10\text{mm}$ in length and gradually increase it to 90 degrees. It can be seen that by increasing the angle of crack, the amount of buckling load of shell is also increased. In figure 6, the diagram shows buckling load variations with angle of crack for a crack with length of $a=10\text{mm}$. For better understanding, these changes are also given in table 1.

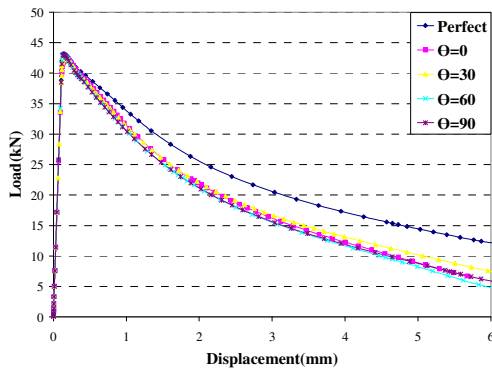


Figure-6

The diagram of buckling load variations vs. crack angle ($a=10\text{ mm}$)

Table-1

The buckling load variations vs. crack angle ($a=10\text{ mm}$)

Buckling Load(kN)	Crack angle(Θ°)
43.168	No crack
42.497	0°
42.690	30°
42.977	60°
43.001	90°

Analyses show that for a crack with the length of 10mm, angle variations don't have any considerable effect on the place of shell buckling. And the shell, by forming the plastic ring in the necking part, will always have symmetrical buckling. In the next step, we double the length of crack and analyze the question with $a=20\text{ mm}$ in different angles.

Load-displacement diagram of these series of shells are shown in figure 7 and their exact values are given in table 2.

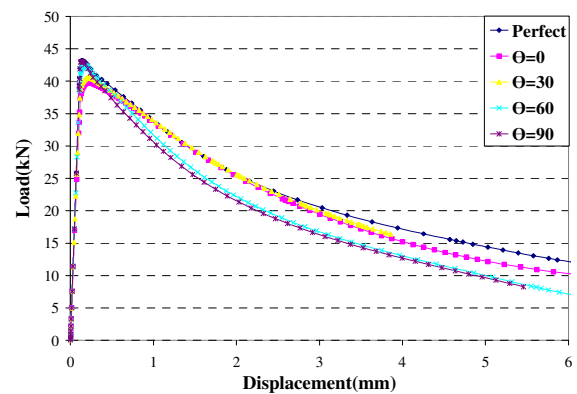


Figure-7

The diagram of buckling load variations vs. crack angle ($a=20\text{ mm}$)

Table-2

The buckling load changes vs. crack angle ($a=20\text{ mm}$)

Buckling Load(kN)	Crack angle(Θ°)
43.168	No crack
39.777	0°
40.535	30°
42.443	60°
43.033	90°

The process of changing shows that by increasing the angle of crack, buckling load is also increased. Because the crack length is raised, these changes are more compared to the shells with crack length of 10 mm. Increasing crack length and parallel to it, reducing shell strength cause that buckling mode of the shell changes and also buckling occurs in an asymmetric mode.

Figure 8 shows buckling of a sample with $a=20\text{ mm}$ and $\Theta=0^\circ$. The reason of choosing a shell with horizontal crack is to show asymmetric buckling of the shell in the situation that geometry has symmetry. In these series of shells, buckling is asymmetric in all crack angles except the one with vertical crack and it is

because of the presence of crack in buckling mode. In continuation, the length of crack is increased to $a=30$ mm. Considering load-displacement diagram in figure 9 and related data table 3, the effect of increasing crack length in parallel with striking reducing of buckling load can be revealed.

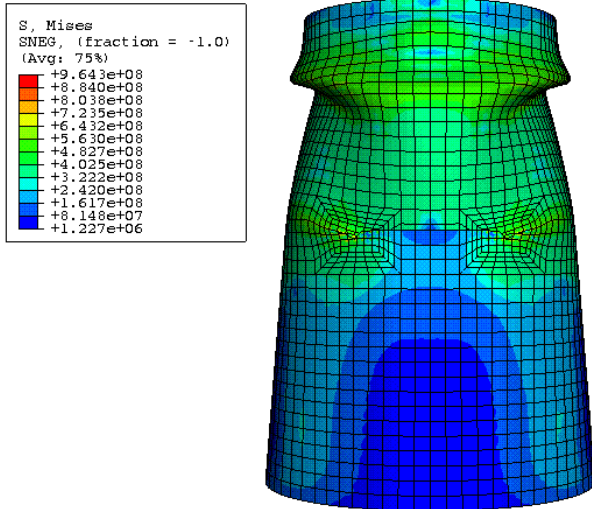


Figure-8
Distributing stress in a shell with $a=2$ mm and $\Theta=0^\circ$

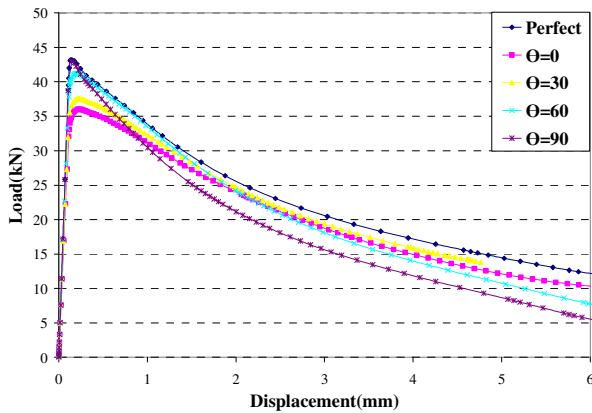


Figure-9
The diagram of buckling load variations vs. crack angle
($a=30$ mm)

Table-3
Buckling load changes vs. crack angle ($a=30$ mm)

Buckling Load(kN)	Crack angle(Θ°)
43.168	No crack
36.024	0°
37.564	30°
41.214	60°
42.970	90°

Figure 10 shows that because of crack geometry, buckling occurs in several areas and also it is completely asymmetric.

In figure 11 the diagram of buckling load variations versus crack length in constant crack angle is depicted. Diagram

reveals that shell buckling load is reduced while crack propagates. Also, horizontal crack has the most significant effect on reducing buckling load of shell while vertical crack has little effect on it.

Analysis of shells 100 mm in height: If the previous process of analysis for shells 100 mm in height is repeated, the graphs similar to previous graphs are obtained. Therefore, only buckling load variations for different crack length with mentioned angles are shown in table 4.

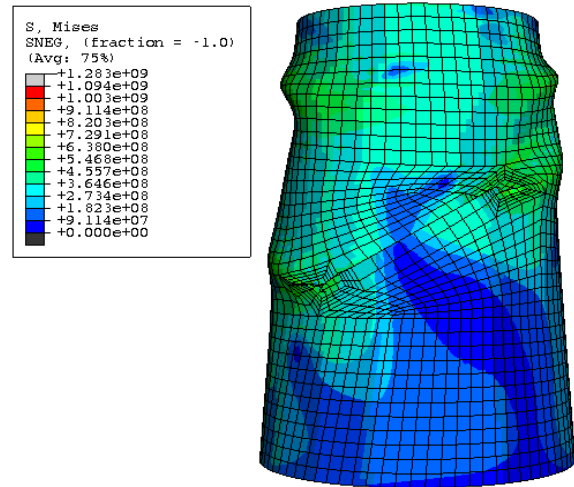


Figure-10
Stress distribution in a shell with $a=30$ mm and $\Theta=30^\circ$

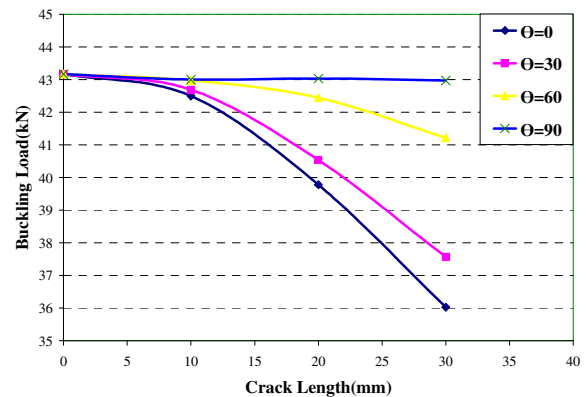


Figure-11
The diagram of buckling load variations vs. crack length in constant crack angles ($H=75$ mm)

Table-4
Buckling load changes vs. crack angle change in different lengths

Buckling Load(kN)			Crack angle(Θ°)
$a=30$ mm	$a=20$ mm	$a=10$ mm	
38.694	38.694	38.694	No crack
33.990	37.304	38.567	0°
35.643	37.759	38.634	30°
38.005	38.495	38.672	60°
38.685	38.686	38.690	90°

It is observed that increasing frusta height strikingly reduces the effect of crack on the buckling load. For example, the most buckling load variations with crack angle, for crack $a=10$ mm in height, has been 0.127 N and for $a=20$ mm, 1.39N and in $a=30$ mm has been 4.704 N. figure 12 demonstrates buckling load variations with crack length in constant crack angles.

In figure 12, it's observed that horizontal crack still has the most significant effect on reducing buckling load and vertical crack doesn't have any considerable effect on buckling load. An Important point in these series of shells is that buckling in all shells is symmetric and leads to make a plastic ring in the necking part of shell with the exception of the shell with $a=30$ mm and $\Theta=30^\circ$ which has asymmetric buckling. For example, figure 13 shows stress distribution in a shell with $a=10$ mm and $\Theta=60^\circ$.

Analysis of shells 150 mm in height: In these series of shells, the effect of height on buckling load is so much that fades greatly the effect of crack and its different angles. For example, from these series of shells, the cracked ones $a=20$ mm in length were studied and its results are mentioned in table 5.

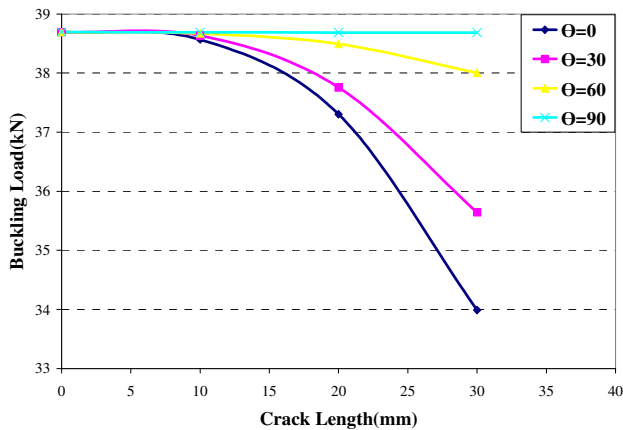


Figure-12

The diagram of buckling load variations vs. crack length in constant crack angles ($H=100$ mm)

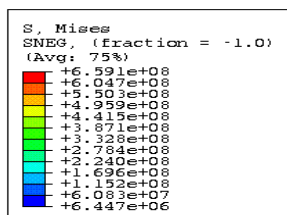


Figure-13

Stress distribution in a shell with $a=10$ mm and $\Theta=60^\circ$

Table-5

Buckling load change vs. crack angle ($a=30$ mm)

Buckling Load(kN)	Crack angle(Θ°)
29.995	No crack
29.738	0°
29.866	30°
29.915	60°
29.976	90°

Table 5 shows that the effect of increasing shell height is so much that buckling load variations as a result of presence of a crack 20 mm in length and different angles is equivalent to 0.257 kN. Because of relatively high height of these series of shells, buckling occurs completely at necking part of shell and creates a symmetrical ring. For instance, buckling of a shell with $a=20$ mm and $\Theta=90^\circ$ is demonstrated in figure 14.

Table 6 indicates the effect of increasing height on buckling load for conical shells with a crack 20 mm in length in different angles. It is observed that in equal loading and support conditions, buckling load is reduced with increasing shell height and also buckling load is raised with increasing crack angle.

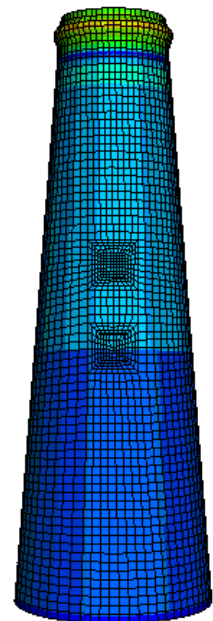
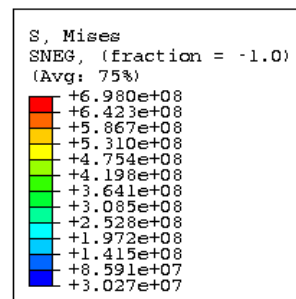


Figure-14

Stress distribution in a shell with $a=20$ mm and $\Theta=90^\circ$

Table-6

Buckling load variations vs. height with presence of a crack with $a=20$ mm and different angles

Buckling Load(kN)				Crack angle(Θ°)
H=150 mm	H=100 mm	H=75 mm		
29.738	37.304	39.777		0°
29.866	37.759	40.535		30°
29.915	38.495	42.443		60°
29.976	38.686	43.033		90°

Table 6 is demonstrated as a diagram in figure 15.

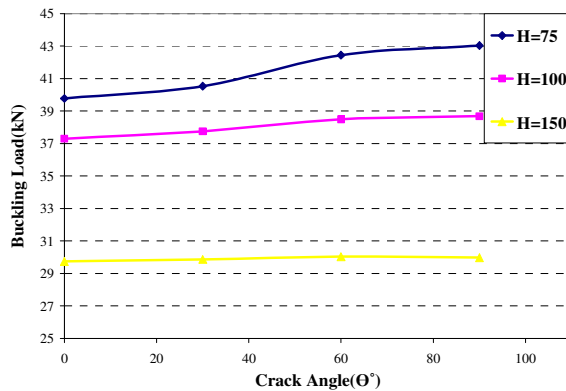


Figure-15

The diagram of buckling load variations vs. crack angles

Comparison of FEM and experimental test results: Different experimental tests were conducted to confirm the authenticity of the results obtained from the numerical method¹⁷⁻²⁰. For example Gupta et al¹⁷ investigated on conical frusta of aluminum of thicknesses between 0.7 and 1.62mm and semi-apical angles range of 16–29° were axially compressed in a universal testing machine. They recorded load–deformation curves and deformed shapes of specimens. All deformation mode of buckling are similar to my investigation and also the behavior of load-displacement was the same.

Conclusion

After buckling phenomenon occurs, load tolerance capacity of shell is severely reduced. The presence of a crack with different angles and obtained stress current has a considerable effect on buckling load of shells. In a constant crack length, with increasing crack angle, buckling load increases and in a constant crack angle, with increasing length, buckling load is reduced. Since vertical crack has little effect on stress current, it isn't so effective on buckling load shell. Where shell at first is buckled depends on several factors. Considering shell geometry, this point may be either in a place that shell has minimum diameter and leads to creating a plastic ring or in a place that as a result of the presence of a crack, plate strength is extremely reduced. In equal loading and support conditions, with increasing shell length, buckling load is considerably reduced. The effect of increasing shell height on buckling load may be to such an extent that the effect of the presence of a crack with definite length is really eliminated; therefore, the effect of the crack presence on buckling load in shells with low height is more noticeable.

References

1. Farshad M., Design and analysis of shell structures, Dordrecht, Kluwer (1992)
2. Shariati M., Fereidoon A. and Akbarpour A., Buckling Load Analysis of oblique Loaded Stainless Steel 316ti

Cylindrical Shells with Elliptical Cutout, *Res. J. Recent Sci.*, **1(2)**, 85-91 (2012)

3. Dadrasi A., An Investigation on Crashworthiness Design of Aluminium Columns with Damage Criteria, *Res. J. Recent Sci.*, **1(7)**, 19-24 (2012)
4. El Naschie MS., Branching solution for local buckling of a circumferentially cracked cylindrical shell, *Int J Mech Sci.*, **16**, 689–97 (1974)
5. Barut A., Madenci A., Britt VO. and Starnes J.H., Buckling of a thin, tensionloaded, composite plate with an inclined crack, *Eng Fract Mech.*, **58**, 233–48 (1977)
6. Riks A., Rankin C.C. and Brogan F.A., The buckling of a central crack in a plate under tension, *Eng Fract Mech.*, **26**, 1023–42 (1992)
7. Chater E. and Hutchinson J.W., On the propagation of bulges and buckles, *J Appl Mech.*, **51**, 1–9 (1984)
8. Starnes J.H. and Rose ChA., A nonlinear response of thin cylindrical shells with longitudinal cracks and subjected to internal pressure and axial compression loads. *Proceedings of the 38th AIAA/ASME/ASCE/AHS/ASC structures, structural dynamics, and materials conference*, 2213–23 (1977)
9. Starnes J.H. and Rose ChA, Buckling and stable tearing responses of unstiffened aluminum shells with long cracks, *AIAA/ASME/ASCE/AHS/ASC structures, structural dynamics and materials conference. Proceedings of the 39th AIAA/ASME/ASCE/AHS/ASC structures, structural dynamics, and materials conference and exhibit and AIAA/ASME/AHS adaptive structures forum*, 2389–402 (1998)
10. Estekanchi H.E. and Vafai A., On the buckling of cylindrical shells with through cracks under axial load, *Thin Wall Struct.*, **35(4)**, 255–74 (1999)
11. Estekanchi H.E., Vafai A. and Kheradmandnia K., Finite element buckling analysis of cracked cylindrical shells under torsion, *Asian J Civ Eng.*, **3(2)**, 73–84 (2002)
12. Vaziri A., On the buckling of cracked composite cylindrical shells under axial compression, *Composite Structures.*, **80**, 152–158, (2007)
13. Postlethwaite H.E. and Mills B., Use of collapsible structural elements as impact isolators with special reference to automotive applications, *J Strain Anal.*, **5**, 58–73 (1970)
14. Mamalis A.G. and Johnson W., The quasi-static crumpling of thin walled circular cylinders and frusta under axial compression, *Int J Mech Sci.*, **25**, 713–32 (1983)
15. Mamalis A.G., Johnson W. and Viegelahn G.L., The crumpling of thin-walled tubes and frusta under axial compression at elevated strain rates, *Int J Mech Sci.*, **26**, 537–47 (1984)

16. ABAQUS 6.4 PR11 user's manual
17. Gupta N.K., Mohamed Sherif N. and Velmurugan R., A study on buckling of thin conical frusta under axial loads, *Thin-Walled Structures*, **44**, 986–996 (2006)
18. Magarajan U., Thundil karuppa Raj R. and Elango T., Numerical Study on Heat Transfer of Internal Combustion Engine Cooling by Extended Fins Using CFD, *Res. J. Recent Sci.*, **1(6)**, 32-37 (2012)
19. Purkar T. Sanjay and Pathak S., Aspect of Finite Element Analysis Methods for Prediction of Fatigue Crack Growth Rate, *Res. J. Recent Sci.*, **1(2)**, 85-91 (2012)
20. Krishan K. and Aggarwal M.L., A Finite Element Approach for Analysis of a Multi Leaf Spring using CAE Tools, *Res. J. Recent Sci.*, **1(2)**, 92-96 (2012)